

EOS Microwave Limb Sounder Observations of “frozen-in” anticyclonic air in Arctic summer

G. L. Manney,^{1,2} N. J. Livesey,¹ C. J. Jimenez,³ H. C. Pumphrey,³ M. L. Santee,¹ I. A. MacKenzie,³ and J. W. Waters¹

Abstract. A previously unreported phenomenon, a “frozen-in” anticyclone (FrIAC) after the 2005 Arctic spring vortex breakup, was discovered in Earth Observing System (EOS) Microwave Limb Sounder (MLS) long-lived trace gas data. A tongue of low-latitude (high-N₂O, low-H₂O) air was drawn into high latitudes and confined in a tight anticyclone, then advected intact in the summer easterlies through late August. A similar feature in O₃ disappeared by early April as a result of chemical processes. The FrIAC was initially advected upright at nearly the same speed at all levels from ~660 to 1300 K (~25–45 km); increasing vertical wind shear after early June tilted the FrIAC and weakened it at higher levels. The associated feature in PV disappeared by early June; transport calculations fail to reproduce the remarkable persistence of the FrIAC, suggesting deficiencies in summer high-latitude winds. The historical PV record suggests that this phenomenon may have occurred several times before. The lack of a persistent signature in O₃ or PV, along with its small size and rapid motion, make it unlikely that a FrIAC could have been reliably identified without hemispheric daily long-lived trace gas profiles such as those from EOS MLS.

1. Introduction

Several modeling studies have examined the evolution of vortex remnants after the springtime breakup. *Hess* [1991] postulated that tracer variations generated during the vortex breakup can be “frozen in”, i.e., remnants of vortex air advected intact by the summer easterlies, in which the shears (horizontal and vertical) are too weak to reduce such anomalies to the fine scale required for them to be dispersed by diffusion. *Orsolini* [2001] showed such Arctic vortex debris persisting into August in a chemical transport model (CTM), noting that long-lived trace gas observations to verify his results were unavailable. *Durry and Hauchecorne* [2005] showed observational evidence, and *Manney et al.* [2005] used long-lived trace gas data from the Earth Observing System (EOS) Microwave Limb Sounder (MLS) to show vortex remnants intact in the middle stratosphere over a month after the 2004 Antarctic vortex breakup.

The Arctic vortex breakup is often triggered by stratospheric sudden warmings. The 2005 vortex broke up in mid-March a “major final warming” (MFW), i.e., a major warming leading directly into the final warming without a intermediate return to westerlies in high latitudes [e.g. *Labitzke and Collaborators*, 2002]. As a result of vigorous wave activity associated with this abrupt final warming, a strong intense anticyclone comprising air drawn up from the tropics formed at high latitude. We detail below EOS MLS long-lived trace gas observations during the vortex breakup and through the summer. In addition to confirmation of frozen-in vortex remnants, these observations show the development and persistence through summer of a strong coherent remnant of air from the high-latitude anticyclone, a phenomenon that has not previously been reported.

We use the first publicly released (v1.51) MLS N₂O, H₂O and O₃ data. Vertical resolution is ~4, 5, and 3 km, and estimated precisions 20–30 ppbv, 0.05–0.1 ppmv, and 0.2–0.3 ppmv, respectively [*Froidevaux et al.*, 2005]. NASA’s Global Modeling and Assimilation Office Goddard Earth Observing System, Version 4.0.3 (GEOS-4) [*Bloom et al.*, 2005], European Centre for Medium Range Weather Fore-

¹Jet Propulsion Laboratory, California Institute of Technology, Pasadena.

²Also at Department of Physics, New Mexico Institute of Mining and Technology.

³University of Edinburgh, UK.

casting (ECMWF), and UK Met Office (MO) meteorological analyses are used to examine winds, potential vorticity (PV), and for transport calculations. Results are shown from the SLIMCAT [Chipperfield, 1999] 3-dimensional (3D) CTM driven with MO winds, run in near real time and sampled at the MLS observation locations.

2. The Evolution of Vortex and Anticyclone Air in Spring and Summer 2005

Figure 1 shows 850 K (~ 10 hPa, ~ 30 km) MLS N_2O and H_2O maps from late March through early August. In the disturbed conditions following the MFW, tongues of low-latitude air are drawn up and entrained into the anticyclone. One such tongue, seen on 24 March, was pulled into a very strong anticyclone at high latitude (e.g., 30 March), bringing with it the high N_2O and low H_2O characteristic of the tropics. After early April, this enclosed air mass was advected intact by the summer easterlies (e.g., 7 April–2 June). While it weakens after early June, the feature is discernible in maps until mid-August. Vortex fragments (also advected by the summer easterlies, but more slowly at their lower latitudes) can be detected through at least mid-July (e.g., near 50°N , 260 – 330°E on 27 April, 200 – 280°E on 2 June, 90 – 140°E on 2 July); later (e.g., 2 August) these are sufficiently diffuse that their identification with vortex air is uncertain. “Frozen-in” vortex remnants have been reported in models [e.g., Hess, 1991; Orsolini, 2001] and observations [e.g., Hess and Holton, 1985; Durry and Hauchecorne, 2005; Manney et al., 2005], and the anticyclonic feature seems to be analogous to these; we refer to it hereinafter as a “frozen-in anticyclone” (FrIAC).

A similar feature forms in O_3 (Figure 2). However, O_3 quickly relaxes to values characteristic of high latitudes; this is similar to the “low-ozone pockets” seen in winter [e.g., Harvey et al., 2004], but relaxation is expected to be even faster in the higher-sunlight springtime conditions. O_3 is the only stratospheric trace gas for which we have previous multiannual hemispheric profile measurements covering Arctic spring and summer. The transience of the FrIAC signature in O_3 therefore suggests that detection of a FrIAC in previous observations was unlikely.

Figure 3 shows Hovmöller (time-longitude) plots of MLS N_2O at 78°N for March through August, at 660 (~ 22 hPa, ~ 25 km), 850, and 1120 K (~ 5 hPa, ~ 40 km). (This and following figures show N_2O ; the same features are apparent in MLS H_2O .) 660 K is near the lowest level at which a persistent FrIAC signature can be seen; 1120 K is near the highest. The FrIAC extends to higher (~ 1400 K) and slightly lower levels (~ 600 K) in April and May, but is not as persistent there. The formation of the FrIAC is seen clearly: The ini-

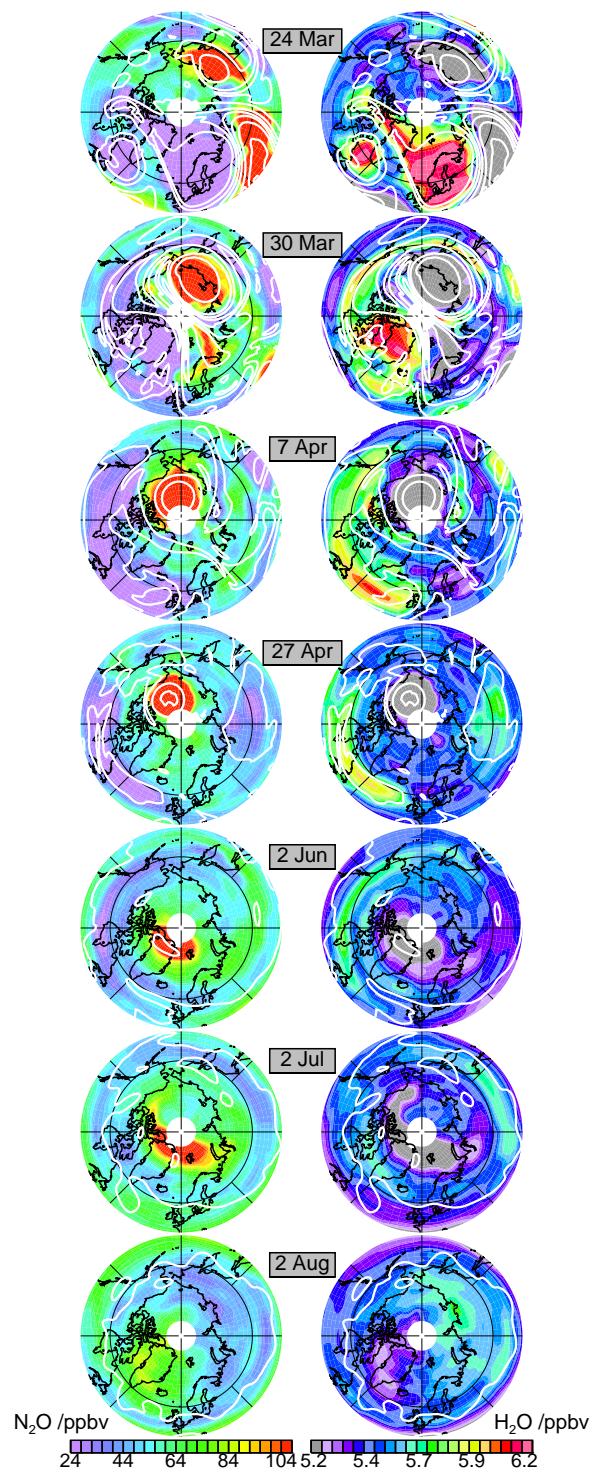


Figure 1. Maps of 850 K MLS N_2O and H_2O after the 2005 Arctic vortex breakup. Overlaid contours are scaled PV (low PV values are associated with high N_2O and low H_2O); fine lines show 60°N latitude.

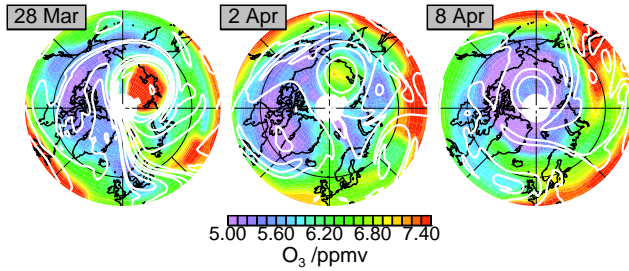


Figure 2. As in Figure 1, but for MLS O_3 in March and early April.

tial high anomaly after ~ 24 March comes from the tongue drawn up from low latitudes. At this time, the background flow is still westerly, and the feature initially moves slowly eastward; in early April (“S” in Figure 3), the mean flow reverses, the FrIAC is advected across the pole (thus, for a short time, ~ 8 – 12 April, not sampled at 78°N), and then advected by the easterlies. Examination of GEOS-4 zonal winds indicates that the period (initially, ~ 23 – 25 days, decreasing to 13–15 days in early May) is consistent with passive advection by the summertime easterlies. The FrIAC period is nearly the same at all levels through early June, consistent with very weak vertical wind shears seen in GEOS-4 in early April–early June at ~ 650 – 1400 K. After early June, vertical wind shear increases below ~ 750 K, and by early July, wind shears are substantial throughout the stratosphere, with weaker (stronger) winds at lower (higher) levels. Consistent with these changing wind shears, the FrIAC period after late June is slower (faster) at lower (higher) levels. The FrIAC can be identified at all three levels through early August as a westward-moving high N_2O feature. At 850 K a distinct signature is seen until late August; during 20–25 August (“F” in Figure 3), 850 K GEOS-4 winds reverse, and the FrIAC stalls and dissipates.

A 3D view of the FrIAC is given in Figure 4; supplementary electronic material contains an animation. The isosurfaces show the deviation in N_2O from a northern hemisphere mean profile averaged over 11 March to 18 July 2005. A larger deviation is used for vortex (low) values, so the vortex does not obscure the view of the FrIAC in its early stages. (Before the FrIAC forms, the animation shows a high N_2O surface apparently descending into the frame; this actually shows air drawn up from low latitudes starting first at higher levels.) As seen in Figure 3, the FrIAC is initially upright, with no longitudinal tilt between levels; this isosurface extends from ~ 650 to 1000 K. After mid-May, the FrIAC begins to tilt and weaken at the higher and lower levels. By mid-June, when vertical wind shears are significant, the FrIAC is strongly tilted westward with height, consistent with stronger easterlies at those levels. Even with the mean

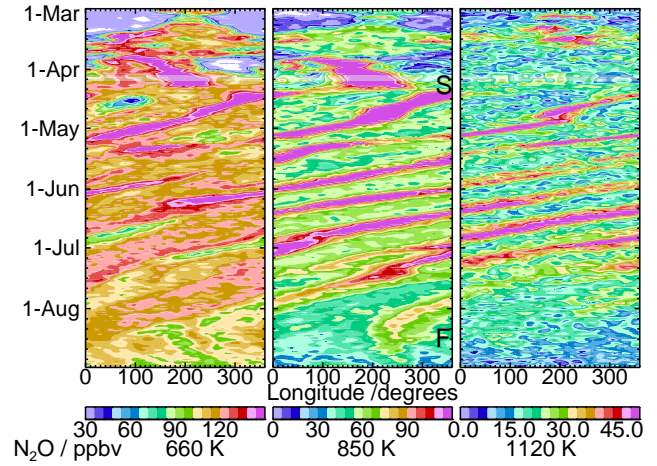


Figure 3. Time-longitude (Hovmöller) plots from March through August 2005 of MLS N_2O at 78°N and (left to right) 660, 850, and 1120 K. Pale stripe shows missing day that has been filled using Kalman smoother. S and F show times of spring and fall background wind reversals at 850 K.

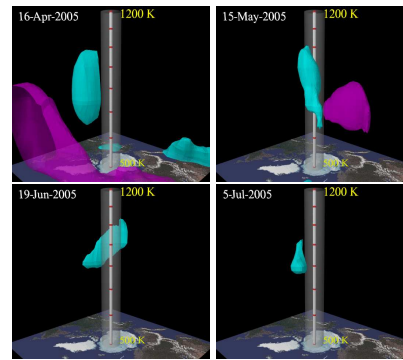


Figure 4. Isosurface plots of N_2O deviations from northern hemisphere mean profile (see text). Cyan surface, $+15$ ppbv, shows anticyclone; magenta surface, -90 ppbv, shows vortex remnant. Vertical range is 500 to 1200 K. Supplementary electronic material contains animation for 1 March–20 July 2005.

removed, it is problematic to choose a single isosurface that captures the FrIAC signature at all levels and times, since strong N_2O gradients also imply differing ranges of variance at different levels. Thus, this isosurface does not extend as high as the FrIAC signature, and while this isosurface disappears around mid-July, the FrIAC signature in the mid-stratosphere persists through most of August (e.g., 850 K in Figure 3).

To explore how the FrIAC is represented in transport models, Figure 5 shows a Hovmöller plot for March through mid-June 2005 of N_2O from the SLIMCAT simulation. Because of deficiencies in initialization and descent in this run, modeled N_2O gradients are weaker and 850 K values lower than those in the MLS data. Still, the formation and initial evolution of the FrIAC are qualitatively the same as in

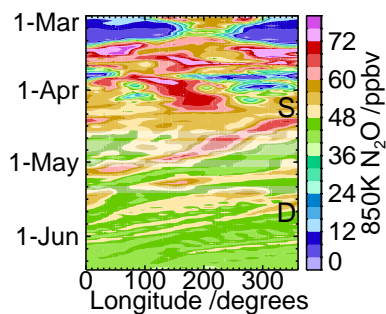


Figure 5. Hovmöller plots at 78°N of SLIMCAT 850 K N₂O from March through mid-June 2005. The contour range is different from that for MLS. Pale stripes show missing days that have been filled with Kalman smoother. S shows spring wind reversal, D time of unrealistic dissipation of FrIAC in model.

the data, with a large high-N₂O anomaly forming, moving slowly eastward until the winds shift in early April (“S” in Figure 5), and then being advected with the easterlies. However, by late May (“D” in Figure 5), the feature in this simulation weakens and disappears. Examination of SLIMCAT maps (not shown) indicates that the feature is unrealistically sheared out after mid-May.

Reverse trajectory (RT) calculations [e.g., Sutton *et al.*, 1994] also reflect unrealistic behavior in modeled transport. RT calculations initialized with MLS N₂O 16 days prior to the dates in Figure 6 show realistic simulation of the FrIAC through early May, but after that the modeled feature is unrealistically shredded, similar to the behavior in SLIMCAT. The 3D SLIMCAT run was driven with MO winds and the MIDRAD radiation scheme for vertical motions; the RT calculations shown here are 3D runs driven with winds and diabatic heating from GEOS-4. 2D (no motion across isentropes) RT runs were also done using MO, ECMWF, and GEOS-4 winds. In each case, unrealistic shredding of the FrIAC commenced at about the same time, though the details of its dissipation differed. The isentropic GEOS-4 runs produced patterns very similar to those in the 3D runs shown here. Consistent results between 3D and isentropic transport calculations using several analyses strongly suggest that the analyzed horizontal winds are unrealistically dispersive at high latitudes in summer. Comparison of the vortex remnants in RT calculations with those in MLS maps suggests that the representation of vortex remnants (at lower latitude in a region of weaker winds) may be more realistic.

3. Discussion and Summary

EOS MLS long-lived trace gas observations have led to the discovery of a previously unreported phenomenon. Following the major final warming in Arctic spring 2005, a

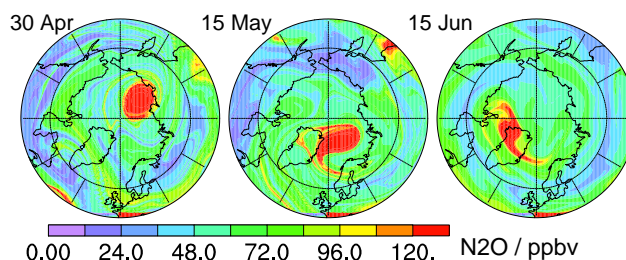


Figure 6. 850 K N₂O maps from 16-day RT calculations (see text) initialized with MLS data, and driven with GEOS-4 winds and diabatic heating rates.

tongue of low-latitude air was drawn into the polar regions and confined in a tight, closed anticyclone. After the prevailing winds reversed several days later, this anticyclonic, low-latitude air was advected intact by the summer easterlies and remained distinct and confined at 70–80°N through late August in the middle stratosphere. The “frozen-in anticyclone” (FrIAC) initially extended from ~660 to 1300 K (~22–3 hPa, ~25–45 km), and was advected at nearly the same speed at all levels through early June. In June and July, vertical wind shears increased, leading to faster advection at higher altitudes, tilting the FrIAC with height and weakening it at higher levels. At 850 K (~10 hPa, ~30 km), the FrIAC persisted through late August, when easterlies weakened and the feature slowed and dissipated. Transport calculations with SLIMCAT, and with a reverse trajectory model driven with several meteorological analyses, fail to reproduce the remarkable persistence of the FrIAC, showing it to shear out and disappear by early June.

The formation and persistence through late May of the anticyclone are seen in PV fields from several analyses, including MO, ECMWF and GEOS-4, but the PV feature disappears in early June. Although this may be partly related to the differing effect of diabatic processes on PV and chemical tracers, the inability of transport calculations to preserve the FrIAC suggests that it may also be related to deficiencies in summer high-latitude horizontal winds, which would be reflected in PV. Previous studies [e.g., Bowman *et al.*, 1998] have found persistent anomalies in summer high-latitude winds in meteorological analyses that may contribute to poor transport model performance.

How common are these occurrences? Unfortunately, the feature is not as persistent in PV, which is the only long-term record for identifying previous occurrences. Also, PV from different analyses varies significantly in its ability to represent the FrIAC, with lower resolution analyses from the MO (more similar to available long-term PV records) providing a less distinct view than those from current ECMWF or GEOS-4 fields. Nevertheless, we have examined the

PV record in spring using MO PV back through 1991 and ECMWF ERA-40 PV back through 1958. We have identified several years in which the PV fields suggest that a FrIAC may have occurred (that is, when a tongue of low latitude air was drawn into a high-latitude anticyclone shortly before the general wind reversal, and a PV signature persisted until late May). The most distinct features were in 1982, 1994 and 2003; 1997 and 2002 PV fields also indicate the possibility of a FrIAC. This suggests that a FrIAC is probably not uncommon, though certainly not an annual phenomenon. Although the Cryogenic Limb Array Etalon Spectrometer (CLAES) on the Upper Atmosphere Research Satellite observed long-lived tracers during parts of spring 1992 and 1993, PV fields in those years do not indicate conditions favorable for a FrIAC to form, and there is no indication of a FrIAC signature in CLAES data. We will look for evidence of a FrIAC in 2003 in Michelson Interferometer for Passive Atmospheric Sounding data. While there may be some evidence of such features in previous sparser datasets (such as those from high-latitude solar occultation instruments), the nature of the FrIAC – the lack of a persistent signature in O₃ or PV, small geographic extent, and rapid motion – is such that it is unlikely that this phenomenon could have been reliably identified without global or hemispheric daily profile measurements of long-lived trace gases such as those from EOS MLS. Identification of the FrIAC phenomenon provides new insight into transport in the spring and summer polar stratosphere, especially the persistence of signatures of winter phenomena, and has the potential to provide information to improve our knowledge of stratospheric winds and our ability to model transport.

Acknowledgments. Thanks to NASA's Global Modeling and Assimilation Office and Steven Pawson for GEOS-4 data and advice on its use, to Kirstin Krüger for assistance with ECMWF data, and to Lucien Froidevaux, Lynn Harvey, and an anonymous reviewer for helpful comments. Work at the Jet Propulsion Laboratory, California Institute of Technology, was done under contract with the National Aeronautics and Space Administration.

References

- Bloom, S. C., et al. (2005), The Goddard Earth Observing Data Assimilation System, GEOS DAS Version 4.0.3: Documentation and validation, *Tech. Rep. 104606 V26*, NASA.
- Bowman, K. P., K. Hoppel, and R. Swinbank (1998), Stationary anomalies in stratospheric meteorological data sets, *Geophys. Res. Lett.*, **25**, 2429–2432.
- Chipperfield, M. P. (1999), Multiannual simulations with a three-dimensional chemical transport model, *J. Geophys. Res.*, **104**, 1781–1805.
- Durry, G., and A. Hauchecorne (2005), Evidence for long-lived polar vortex air in the mid-latitude summer stratosphere from in situ laser diode CH₄ and H₂O measurements, *Atmos. Chem. Phys.*, **5**, 1467–1472.
- Froidevaux, L., et al. (2005), Early validation analyses of atmospheric profiles from EOS MLS on the Aura satellite, *IEEE Trans. Geosci. Remote Sens.*, in press, 2005.
- Harvey, V. L., et al. (2004), On the distribution of ozone in stratospheric anticyclones, *J. Geophys. Res.*, **109**, D24308, doi:10.1029/2004JD004992.
- Hess, P. G. (1991), Mixing processes following the final stratospheric warming, *J. Atmos. Sci.*, **48**, 1625–1641.
- Hess, P. G., and J. R. Holton (1985), The origin of temporal variance in long-lived trace constituents in the summer stratosphere, *J. Atmos. Sci.*, **42**, 1455–1463.
- Labitzke, K., and Collaborators (2002), *The Berlin Stratospheric Data Series*, CD from Meteorological Institute, Free University Berlin, Berlin, Germany.
- Manney, G. L., et al. (2005), EOS Microwave Limb Sounder observations of the Antarctic polar vortex breakup in 2004, *Geophys. Res. Lett.*, **32**, L12811, doi:10.1029/2005GL022823.
- Orsolini, Y. J. (2001), Long-lived tracer patterns in the summer polar stratosphere, *Geophys. Res. Lett.*, **28**, 3855–3858.
- Sutton, R. T., et al. (1994), High-resolution stratospheric tracer fields estimated from satellite observations using Lagrangian trajectory calculations, *J. Atmos. Sci.*, **51**, 2995–3005.
- G. L. Manney (corresponding author), Department of Physics, New Mexico Institute of Mining and Technology, Socorro, NM 87801. (e-mail: manney@mls.jpl.nasa.gov)
- N. J. Livesey, M. L. Santee, J. W. Waters, Jet Propulsion Laboratory, Mail Stop 183–701, 4800 Oak Grove Drive, Pasadena, CA 91109.
- C. Jimenez, H. C. Pumphrey, School of GeoSciences, The University of Edinburgh, Edinburgh EH9 3JN, UK.

This preprint was prepared with AGU's L^AT_EX macros v4, with the extension package 'AGU⁺⁺' by P. W. Daly, version 1.6b from 1999/08/19.